A New Rainbow: Angular Scattering of the F + $H_2(v_i = 0, j_i = 0) \rightarrow FH(v_f = 3, j_f = 3) + H$ Reaction†

Chengkui Xiahou and J. N. L. Connor*

School of Chemistry, The University of Manchester, Manchester M13 9PL, England

Received: June 28, 2009; Revised Manuscript Received: September 11, 2009

The angular scattering of a state-to-state chemical reaction contains fundamental information on its dynamics. Often the angular distributions are highly structured and the physical interpretation of this structure is an important and difficult problem. Here, we report a surprising finding for the benchmark F + $H_2 \rightarrow$ FH + H reaction, when the product molecule FH is in a vibrational state with quantum number = 3 and a rotational state with quantum number = 3. We demonstrate that the differential cross section (DCS) is an example of (attractive) rainbow scattering, being characterized by an Airy function and its derivative. The rainbow reveals its presence in the DCS by interference with the repulsive (or nearside) scattering producing characteristic diffraction oscillations. The rainbow is broad, which explains why it has not been recognized in the many earlier theoretical and experimental investigations of this reaction. There is an angular region in the DCS where the rainbow dominates, but with the unusual property that the DCS is less intense than in adjoining angular regions. The reaction investigated is F + $H_2(v_i = 0, j_i = 0, m_i = 0) \rightarrow FH(v_f = 3, j_f = 3, m_f = 0)$ + H, where v_i, j_i, m_i and v_f, j_f, m_f are initial and final vibrational, rotational and helicity quantum numbers, respectively. The relative translational energy is 0.119 eV. We use rigorous semiclassical (asymptotic) techniques that provide physical insight as well as a mathematically sound and numerically accurate description of the angular scattering. The semiclassical DCS agrees very closely with the exact quantum DCS. The semiclassical scattering amplitude is used to assess the physical effectiveness of the Fuller nearside−farside decomposition for the partial wave series of the F + H_2 reaction, including the effect of one resummation. We also compare the semiclassical and exact quantum nearside, farside, and full local angular momenta and find good agreement. Although our new rainbow has unusual and unexpected properties, similar rainbows are predicted to occur in the DCSs of many state-to-state chemical reactions, since the semiclassical analysis is generic and not specific to the present F + H_2 example.

1. Introduction

Understanding the dynamics of chemical reactions is a subject of fundamental importance in chemistry. Experiments can now measure state-to-state angular distributions over an extended energy range.[1] In addition, there have been significant developments in computational algorithms for quantum reactive scattering in the energy and time domains that are producing a wealth of important numerical data. The most recent review of theories of quantum reactive scattering is that by Hu and Schatz[2] in 2006, which discusses about 600 papers published during the last 20 years or so. Some more recent quantum calculations of differential cross sections for chemical reactions can be found in refs 3−23.

Hu and Schatz comment that experiments have often produced a wealth of data that theorists have taken decades to understand, that new computations have frequently resulted in "confusions" in their interpretation, and that many challenges remain for theory.[2] These comments certainly apply to the state-to-state F + $H_2 \rightarrow$ FH + H reaction, which has played a key role in understanding the dynamics of exoergic reactions. It has been extensively studied by theory and experiment for more than 40 years.[1,2] Of particular interest has been the angular scattering associated with the FH ($v_f = 3$) vibrational state, as first measured in the classic crossed molecular-beam experiments of Neumark et al.[24] and more recently by Wang et al.[25]

The purpose of this paper is to report a surprising new finding for the dynamics of the F + H_2 reaction: We demonstrate that the angular scattering of the FH ($v_f = 3$) product is an example of (attractive) *rainbow scattering*. We prove this result by taking the semiclassical (i.e., asymptotic) limit of the (farside) scattering amplitude and showing that it is characterized by an Airy function and its first-order derivative. In particular, there is a transition from the bright side of the rainbow to its dark side as the reactive scattering angle increases. The rainbow is broad, which explains why it has not been recognized in the many earlier theoretical and experimental investigations. The rainbow also reveals its presence by interference with the repulsive (or nearside) scattering producing characteristic diffraction oscillations in the differential cross section. We show there is an angular region in the differential cross section where the rainbow dominates, but with the unusual property that it is less intense than in adjoining angular regions.

An important point is that we use rigorous semiclassical techniques that provide a mathematically sound and numerically accurate description of the angular scattering and avoid subjective interpretations. We refer to refs 26−31 for information on the semiclassical techniques that we employ. These include the asymptotic approximation of Legendre polynomials, the Poisson series representation of the scattering amplitude, and the uniform stationary phase evaluation of oscillating integrals. In addition,

† Part of the "Vincenzo Aquilanti Festschrift".

* Corresponding author. E-mail: j.n.l.connor@manchester.ac.uk.

10.1021/jp906042g
Published on Web 11/12/2009

we refer to a recent review by Adam[32] for an account of the theory of rainbows at different levels of mathematical sophistication; this review also describes many physical applications of rainbow theory.

In the following, we consider the state-to-state reaction

$$F + H_2\,(v_i = 0, j_i = 0, m_i = 0) \rightarrow FH\,(v_f = 3, j_f = 3, m_f = 0) + H$$

where v_i, j_i, m_i and v_f, j_f, m_f are initial and final vibrational, rotational and helicity quantum numbers respectively. The relative translational energy is 0.119 eV, which corresponds to a total energy of $E = 0.3872$ eV measured with respect to the minimum of the H_2 potential energy curve. This combination of collision parameters is an important contributor to the experiment of Neumark et al.[24] We denote the reactive scattering angle by θ_R; that is, the angle between the outgoing FH molecule and the incoming F atom in the center-of-mass collision frame.

Section 2 outlines the theoretical methods used. We begin with the partial wave series representation of the scattering amplitude and its decomposition into *nearside* and *farside* subamplitudes. We also discuss the resummation of the partial wave series prior to making the nearside−farside decomposition. We also consider the related topic of nearside and farside *local angular momenta*. Section 3 describes the rainbow that occurs in the angular scattering of the $F + H_2$ reaction and discusses its properties. Section 4 contains our conclusions.

2. Theory

Our starting point is the reactive scattering amplitude, $f(\theta_R)$ for which the corresponding differential cross section (DCS) is given by

$$\sigma(\theta_R) = |f(\theta_R)|^2 \tag{1}$$

We first consider the partial wave series (PWS) representation for $f(\theta_R)$, then its semiclassical (SC) limit. An important technique we apply to both the PWS and SC representations of $f(\theta_R)$ is that of nearside−farside (NF) analysis,[33−61] which has been reviewed in refs 58 and 62−64. Other recent applications of NF theory can be found in refs 65−85.

A. Partial Wave Theory. ***(a) Scattering Amplitude and Nearside-Farside Decomposition.*** Since the helicity quantum numbers are both zero, we can expand $f(\theta_R)$ in a basis set of Legendre polynomials, thereby obtaining the PWS representation for $f(\theta_R)$. We have

$$f(\theta_R) = (2ik)^{-1} \sum_{J=0}^{\infty} (2J + 1)\tilde{S}_J P_J(\cos\theta_R) \tag{2}$$

where k is the initial translational wavenumber, J is the total angular momentum quantum number, $\tilde{S}_J$ is the Jth modified scattering matrix element, and $P_J(\bullet)$ is a Legendre polynomial of degree J. For notational simplicity, the label v_i, j_i, $m_i \rightarrow v_f$, j_f, m_f has been omitted from $f(\theta_R)$ and $\tilde{S}_J$, as has the label v_i, j_i from k. Below, we discuss a resummation of the PWS, then we write eq 2 in the more compact form

$$f(\theta_R) = (2ik)^{-1} \sum_{J=0}^{\infty} a_J P_J(\cos\theta_R) \tag{3}$$

where $a_J = (2J + 1)\tilde{S}_J$. Under semiclassical conditions, the PWS in eqs 2 or 3 contains a large number of partial waves, typically of order kR, where R is the reaction radius.

We will find in Section 3 that $\sigma(\theta_R)$ is structured and that the structure contains important information on the dynamics of the reaction. For this situation, it is helpful to make a NF decomposition of $f(\theta_R)$. We write[33−61]

$$f(\theta_R) = f_N(\theta_R) + f_F(\theta_R) \tag{4}$$

where the N, F subamplitudes are given by ($\theta_R \neq 0, \pi$)

$$f_{N,F}(\theta_R) = \frac{1}{2ik} \sum_{J=0}^{\infty} (2J + 1)\tilde{S}_J Q_J^{(N,F)}(\cos\theta_R) \tag{5}$$

with[86]

$$Q_J^{(N,F)}(\cos\theta_R) = \frac{1}{2}\left[P_J(\cos\theta_R) \pm \frac{2i}{\pi} Q_J(\cos\theta_R)\right] \tag{6}$$

and $Q_J(\bullet)$ is a Legendre function of the second kind of degree J. The corresponding N, F DCSs are then

$$\sigma_N(\theta_R) = |f_N(\theta_R)|^2 \tag{7}$$

and

$$\sigma_F(\theta_R) = |f_F(\theta_R)|^2 \tag{8}$$

respectively.

We will also discuss in Section 3 the full and N, F local angular momenta (LAMs) for the reaction.[49,50,52,55−61,73] The full LAM is defined by

$$\mathrm{LAM}(\theta_R) = \frac{d\arg f(\theta_R)}{d\theta_R} \tag{9}$$

and the corresponding N, F LAMs by

$$\mathrm{LAM}_{N,F}(\theta_R) = \frac{d\arg f_{N,F}(\theta_R)}{d\theta_R} \tag{10}$$

In eqs 9 and 10, the arg is not necessarily the principal value in order that the derivatives be well-defined.

(b) Resummation of the Scattering Amplitude and Nearside−Farside Decomposition. We also investigate how the NF DCSs change upon resumming the PWS in eq 2, since it is known that a resummation can improve the physical effectiveness of a NF decomposition.[41,42,46,48−50,52,56,58,59] By "resummation", we mean a rearrangement of the terms in a PWS to give a new series in which the new terms have more desirable properties. A spectacular example concerns scattering for a Coulomb potential, for which the PWS is divergent, whereas the resummed series is convergent. This example is discussed in ref 49.

For one resummation, denoted $R = 1$, the resummed scattering amplitude has the representation[49]

$$f(\theta_R) = \frac{1}{2ik}\frac{1}{1+\beta_1\cos\theta_R}\sum_{J=0}^{\infty} a_J^{(1)}(\beta_1)\, P_J(\cos\theta_R) \tag{11}$$

where

$$a_J^{(1)}(\beta_1) = \beta_1\frac{J}{2J-1}a_{J-1} + a_J + \beta_1\frac{J+1}{2J+3}a_{J+1} \qquad J = 0, 1, 2, \ldots \tag{12}$$

with $a_{-1} = 0$. Equation 11 also assumes that $1 + \beta_1 \cos\theta_R \neq 0$. We determine the complex valued parameter, β_1, in eqs 11 and 12 by solving $a_{J=0}^{(1)}(\beta_1) = 0$, which yields $\beta_1 = -3a_0/a_1$. For the results in Section 3, we find $\beta_1 = 0.999 + 0.166i$. A NF decomposition of eq 11 can also be made. We write

$$f(\theta_R) = f_N(\beta_1;\theta_R) + f_F(\beta_1;\theta_R) \tag{13}$$

where the N, F $R = 1$ resummed subamplitudes are given by ($\theta_R \neq 0, \pi$)

$$f_{N,F}(\beta_1;\theta_R) = \frac{1}{2ik}\frac{1}{1+\beta_1\cos\theta_R}\sum_{J=0}^{\infty} a_J^{(1)}(\beta_1)\, Q_J^{(N,F)}(\cos\theta_R) \tag{14}$$

The corresponding N, F $R = 1$ resummed DCSs are then

$$\sigma_N(\beta_1;\theta_R) = |f_N(\beta_1;\theta_R)|^2 \tag{15}$$

and

$$\sigma_F(\beta_1;\theta_R) = |f_F(\beta_1;\theta_R)|^2 \tag{16}$$

respectively. NF LAMs for $R = 1$ can also be defined by analogy with eq 10; namely,

$$\mathrm{LAM}_{N,F}(\beta_1;\theta_R) = \frac{d\arg f_{N,F}(\beta_1;\theta_R)}{d\theta_R} \tag{17}$$

Note that the full DCSs and LAMs for $R = 0$ and $R = 1$ are numerically identical.

We will use the notation $R = 0$ to indicate the unresummed formulas of eqs 1−10.

B. Semiclassical Theory. ***(a) Definitions.*** This section derives the F and N semiclassical subamplitudes, $f_{\pm}^{SC}(\theta_R)$ and $f_{-}^{SC}(\theta_R)$, respectively,[26−31,52] whose sum gives the SC approximation to the full scattering amplitude

$$f^{SC}(\theta_R) = f_{+}^{SC}(\theta_R) + f_{-}^{SC}(\theta_R) \tag{18}$$

Notice that we use ± to label the F and N SC subamplitudes, respectively, to avoid confusion with the PWS $f_{F,N}(\theta_R)$ and $f_{F,N}(\beta_1;\ \theta_R)$ defined by eqs 5 and 14, respectively. The corresponding full SC DCS is

$$\sigma^{SC}(\theta_R) = |f^{SC}(\theta_R)|^2 \tag{19}$$

and the F and N SC DCSs are given by

$$\sigma_{\pm}^{SC}(\theta_R) = |f_{\pm}^{SC}(\theta_R)|^2 \tag{20}$$

The full SC LAM is defined by

$$\mathrm{LAM}^{SC}(\theta_R) = \frac{d\arg f^{SC}(\theta_R)}{d\theta_R} \tag{21}$$

The F, N SC LAMs are defined in a way analogous to eq 21.

(b) Semiclassical Poisson Representation for the Scattering Amplitude. We now begin the SC derivation. Since we are not concerned with scattering into the angles $\theta_R = 0$ and $\theta_R = \pi$, the *first* step[26−31,52] in our SC analysis is to approximate the Legendre polynomials in the PWS in eq 2 as the sum of two traveling angular waves.

$$P_{\lambda-1/2}(\cos\theta_R) \sim \left[\frac{1}{2\pi\lambda\sin\theta_R}\right]^{1/2}\left\{\exp\left[i\left(\lambda\theta_R - \frac{1}{4}\pi\right)\right] + \exp\left[-i\left(\lambda\theta_R - \frac{1}{4}\pi\right)\right]\right\} \tag{22}$$

where $\lambda = J + 1/2$. The SC (or asymptotic) approximation in eq 22 is valid for $\lambda \sin\theta_R \gg 1$. If the approximation in eq 22 is used in eq 2, the exact and approximate DCSs are expected to be almost indistinguishable, except for angles close to 0 and π. We have confirmed this well-known result for the F + H_2 reaction. Note that the approximation in eq 22 is also the first step in Brink's extensive development of semiclassical collision theory in his monograph (ref 28, p 53). All semiclassical approximations in the following based on eq 22 will begin with the label "SC".

In the *second* step,[26−31,52] we apply the Poisson sum formula and assume that real stationary phase points occur only in the leading term, $m = 0$ (see below for the justification of this assumption for the F + H_2 reaction). This lets us write the resulting $f^{SC}(\theta_R)$, for $\theta_R \neq 0, \pi$ as the sum of F and N subamplitudes, $f_{+}^{SC}(\theta_R) + f_{-}^{SC}(\theta_R)$, where[52]

$$f_{\pm}^{SC}(\theta_R) = \frac{1}{ik}\frac{1}{(2\pi\sin\theta_R)^{1/2}}\exp\left(\mp i\frac{1}{4}\pi\right)I_{\pm}(\theta_R) \tag{23}$$

with

$$I_{\pm}(\theta_R) = \int_0^{\infty} d\lambda\lambda^{1/2}|\tilde{S}(\lambda)|\exp\{i[\arg\tilde{S}(\lambda) \pm \lambda\theta_R]\} \tag{24}$$

In eq 24, $\tilde{S}(\lambda) \equiv \tilde{S}_{\lambda-1/2} = \tilde{S}_J = \tilde{S}(J)$ has been continued to continuous values from half-integer values of $\lambda = 1/2, 3/2, 5/2, \ldots$. We will refer to eqs 23 and 24 as SC Poisson ($m = 0$) representations of $f_{\pm}^{SC}(\theta_R)$ and use the notations SC/F/Poisson and SC/N/Poisson for the F and N contributions, respectively.

(c) Stationary Phase Condition. The *third* and crucial step applies uniform stationary phase techniques to the $I_{\pm}(\theta_R)$ to extract their physical content.[26−31,52] Assuming that $|\tilde{S}(\lambda)|$ is slowly varying in eq 24, the *stationary phase condition* is

$$\frac{d}{d\lambda}[\arg\tilde{S}(\lambda) \pm \lambda\theta_R] = 0 \tag{25}$$

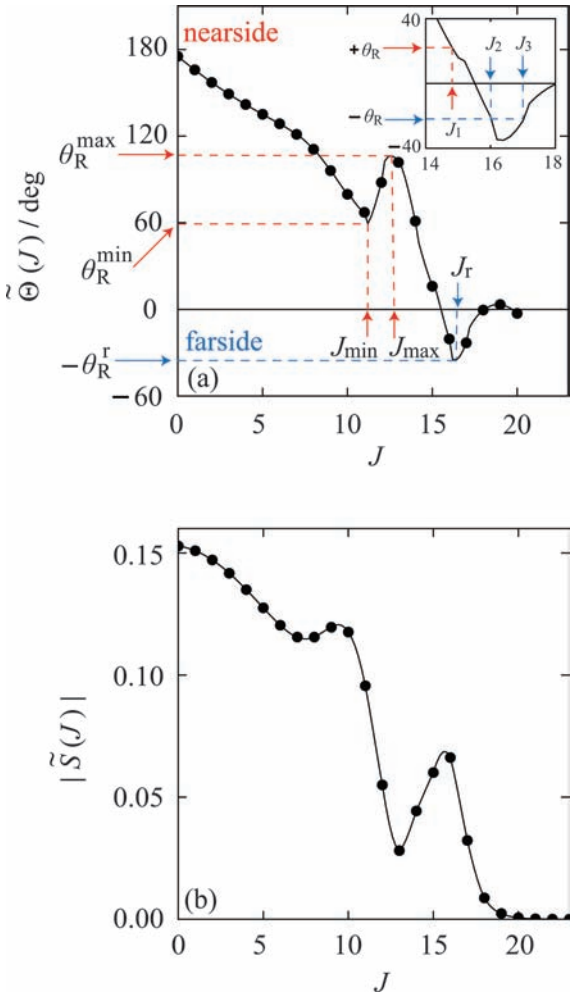

Figure 1. (a) Plot of the quantum deflection function, $\tilde{\Theta}(J)$, vs J. The solid circles indicate integer values of J. The red dashed lines and red arrows indicate θ_R^{min}, θ_R^{max} and J_{min}, J_{max} for the nearside scattering; the blue dashed lines and blue arrows indicate $-\theta_R^r$ and J_r for the farside scattering. The inset shows the labeling of the stationary phase points, J_1, J_2, J_3 that is used when $\theta_R < \theta_R^r$ in the SC theory. (b) Plot of $|\tilde{S}(J)|$ vs J. The solid circles indicate integer values of J.

Equation 25 can be written in the alternative form[51,52]

$$\tilde{\Theta}(\lambda) = \mp\theta_R \tag{26}$$

where we have introduced the *quantum deflection function*, $\tilde{\Theta}(\lambda) \equiv$ d arg $\tilde{S}(\lambda)$/dλ; it plays a fundamental role in the following.

To continue with the SC analysis, it is first essential to examine the properties of $\tilde{\Theta}(\lambda)$ [or equivalently, $\tilde{\Theta}(J)$]. Figure 1 plots graphs of $\tilde{\Theta}(J)$ vs J and also $|\tilde{S}(J)|$ vs J for the F + H_2 reaction. Our labeling for the real roots of eq 26 is also defined in Figure 1a. A classical-like *rainbow singularity* occurs at angles where d $\tilde{\Theta}(J)$/d$J = 0$. Figure 1a shows there are three rainbow singularities: one in the F scattering at $\tilde{\Theta}(J) = -\theta_R^r$ and two in the N scattering at $\tilde{\Theta}(J) = +\theta_R^{min}$ and $\tilde{\Theta}(J) = +\theta_R^{max}$. Note that the three rainbow angles and $\tilde{\Theta}(J)$ have values between $-180°$ and $+180°$, which justifies keeping the leading term of the Poisson sum ($m = 0$) in the second step of the SC analysis.

We will discuss the evaluation of the F and N SC subamplitudes separately.

(d) Semiclassical Rainbow Analysis of the Farside Scattering. The plot of $\tilde{\Theta}(J)$ vs J in Figure 1a has a minimum at $\tilde{\Theta}(J) = -\theta_R^r = -35.2°$ where $J = J_r = 16.3$. Note that a (nonuniform) primitive stationary phase approximation (PSA)[51] applied to the integral $I_+(\theta_R)$ in eq 24 would be divergent at the rainbow angle.

We first consider the *bright side* of the rainbow, where $\theta_R < \theta_R^r$, and the stationary phase condition,

$$\tilde{\Theta}(J) = -\theta_R \tag{27}$$

has two simple real roots that coalesce at $\theta_R = \theta_R^r$. We denote the two real roots of eq 27 by $J_2(\theta_R)$ and $J_3(\theta_R)$. They are illustrated in the inset to Figure 1a. Equivalently, in λ space, we have $\tilde{\Theta}(\lambda) = -\theta_R$ for $\lambda = \lambda_2(\theta_R)$ and $\lambda = \lambda_3(\theta_R)$.

The *uniform Airy approximation* is obtained when the oscillating integral $I_+(\theta_R)$ in eq 24 is evaluated by (uniform) asymptotic techniques that allow for two real coalescing stationary phase points.[87] The uniform SC approximation for this situation is given in the Appendix. Applying eqs A.2−A.4 to eqs 23 and 24, we obtain the following result for the uniform Airy approximation when $\theta_R \le \theta_R^r$

$$f_+^{uAiry}(\theta_R) = \pi^{1/2} \exp\{i[A(\theta_R) - 3\pi/4]\} \times \{[\sigma_2(\theta_R)^{1/2} + \sigma_3(\theta_R)^{1/2}]\varsigma(\theta_R)^{1/4}\, \mathrm{Ai}(-\varsigma(\theta_R)) + i[\sigma_2(\theta_R)^{1/2} - \sigma_3(\theta_R)^{1/2}]\, \varsigma(\theta_R)^{-1/4}\, \mathrm{Ai}'(-\varsigma(\theta_R))\} \tag{28}$$

where

$$A(\theta_R) = \frac{1}{2}\{\arg \tilde{S}(\lambda_2(\theta_R)) + \arg \tilde{S}(\lambda_3(\theta_R)) + [\lambda_2(\theta_R) + \lambda_3(\theta_R)]\theta_R\} \tag{29}$$

and

$$\varsigma(\theta_R) = \left[\frac{3}{4}\{\arg \tilde{S}(\lambda_2(\theta_R)) - \arg \tilde{S}(\lambda_3(\theta_R)) + [\lambda_2(\theta_R) - \lambda_3(\theta_R)]\theta_R\}\right]^{2/3} \tag{30}$$

Note that $\varsigma(\theta_R) \ge 0$. The prime on the Airy function, Ai′(x), means d Ai(x)/dx. The "classical-like" DCSs, $\sigma_2(\theta_R)$ and $\sigma_3(\theta_R)$, in eq 28 are defined by

$$\sigma_i(\theta_R) = \frac{\lambda_i(\theta_R)|\tilde{S}(\lambda_i(\theta_R))|^2}{k^2 \sin\theta_R \left|\frac{d\tilde{\Theta}(\lambda)}{d\lambda}\right|_{\lambda=\lambda_i(\theta_R)}} \qquad i = 2, 3 \tag{31}$$

Equations 28−31 are valid on the bright side of the rainbow and depend only on the properties of $\tilde{S}(\lambda)$ at $\lambda = \lambda_2(\theta_R)$ and $\lambda = \lambda_3(\theta_R)$. The *principle of asymptotic equivalence* tells us that the integral representation, SC/F/Poisson [i.e., eqs 23 and 24], and the uniform Airy result (28) are equivalent under semiclassical conditions, $kR \gg 1$. However a numerical evaluation of eqs 23 and 24 by quadrature provides us with no physical insight, in contrast to eqs 28−31, which show that the F scattering is an example of an (attractive) Airy rainbow. We will use the notation SC/F/uAiry for eqs 28−31.

We now consider the *dark side* of the rainbow, where $\theta_R > \theta_R^r$. The roots of the stationary phase condition $\tilde{\Theta}(J) = -\theta_R$ become complex valued, which are awkward to handle when

dealing with numerical input data. To avoid this problem, we use a *transitional Airy approximation*,[87] which is equivalent to making a quadratic approximation for $\tilde{\Theta}(\lambda)$ about $\lambda = \lambda_r$; namely,

$$\tilde{\Theta}(\lambda) \approx -\theta_R^r + q_r(\lambda - \lambda_r)^2 \quad \text{where} \quad q_r = \frac{1}{2}\frac{d^2\tilde{\Theta}(\lambda)}{d\lambda^2}\bigg|_{\lambda=\lambda_r} \tag{32}$$

with $\lambda_r = J_r + 1/2 = 16.8$ and $q_r = 0.606$ rad. Applying eq A.5 of the Appendix to eqs 23 and 24, we obtain

$$f_+^{tAiry}(\theta_R) = \frac{1}{k}\left(\frac{2\pi\lambda_r}{\sin\theta_R}\right)^{1/2}\frac{|\tilde{S}(\lambda_r)|}{q_r^{1/3}}\exp\{i[\arg\tilde{S}(\lambda_r) + \lambda_r\theta_R - 3\pi/4]\} \times \left\{\mathrm{Ai}\left(\frac{\theta_R - \theta_R^r}{q_r^{1/3}}\right) - \frac{i}{q_r^{1/3}}\left[\frac{1}{2\lambda_r} + \frac{1}{|\tilde{S}(\lambda_r)|}\frac{d|\tilde{S}(\lambda)|}{d\lambda}\bigg|_{\lambda=\lambda_r}\right]\mathrm{Ai}'\left(\frac{\theta_R - \theta_R^r}{q_r^{1/3}}\right)\right\} \tag{33}$$

We will use the abbreviation SC/F/tAiry for eqs 32 and 33. Notice that eq 33 depends only on the properties of $\tilde{S}(\lambda)$ at $\lambda = \lambda_r = \lambda_r(\theta_R^r)$ and can be used on both the bright and dark sides of the rainbow, as well as at $\theta_R = \theta_R^r$. However, eq 33 is expected to be most reliable for $\theta_R \approx \theta_R^r$, where the Taylor expansion in the approximate eq 32 is most accurate. The dominant contribution to $f_+^{tAiry}(\theta_R)$ comes from the Ai(•) term in eq 33.

Also note the limit

$$\lim_{\theta_R \to \theta_R^r} f_+^{uAiry}(\theta_R) = f_+^{tAiry}(\theta_R^r) \tag{34}$$

Equation 34 is an important result, since eq 28 is numerically indeterminate, 0/0, at $\theta_R = \theta_R^r$ (= 35.2°) and in practice becomes numerically unstable for $\theta_R \approx \theta_R^r$. To avoid these numerical problems, $f_+^{uAiry}(\theta_R)$ is used for $\theta_R \le 30°$, and $f_+^{tAiry}(\theta_R)$, for $\theta_R > 30°$ in the calculations described in Section 3.

(e) Semiclassical Analysis of the Nearside Scattering. Finally, we consider the N SC subamplitude, $f_-^{SC}(\theta_R)$, which has the Poisson representation, SC/N/Poisson, of eqs 23 and 24. The stationary phase condition for the integral $I_-(\theta_R)$ in eq 24 is now

$$\tilde{\Theta}(\lambda) = +\theta_R \tag{35}$$

Figure 1a shows there are two rainbow singularities in the N scattering: at $\tilde{\Theta}(J) = +\theta_R^{min} = 57.1°$ for $J = J_{min} = 11.0$ and $\tilde{\Theta}(J) = +\theta_R^{max} = 106.5°$ for $J = J_{max} = 12.6$. Then for $\theta_R^{min} \le \theta_R \le \theta_R^{max}$, there are *three* real stationary phase points, two of which coalesce at $\theta_R = \theta_R^{min}$, and two coalesce when $\theta_R = \theta_R^{max}$. This situation corresponds semiclassically to the *uniform Pearcey approximation*.[88] Formally, we can write the asymptotic relation

$$f_-^{SC}(\theta_R) \sim \text{uniform Pearcey semiclassical approximation} \tag{36}$$

The principle of asymptotic equivalence again tells us that the SC/N/Poisson representation (i.e., eqs 23 and 24) and the uniform Pearcey result of eq 36 are equivalent under semiclassical conditions, $kR \gg 1$. Now if the three real stationary phase points for $\theta_R^{min} < \theta_R < \theta_R^{max}$ make comparable contributions to $f_-^{SC}(\theta_R)$, then we might expect an intense interference structure in this angular range (for an example, see Figure 10 of ref 88 in a model curve-crossing study of $He^+ + Ne$ scattering). However, we will see in Section 3 that this is not the case; rather, the inner stationary phase point makes the dominant contribution.

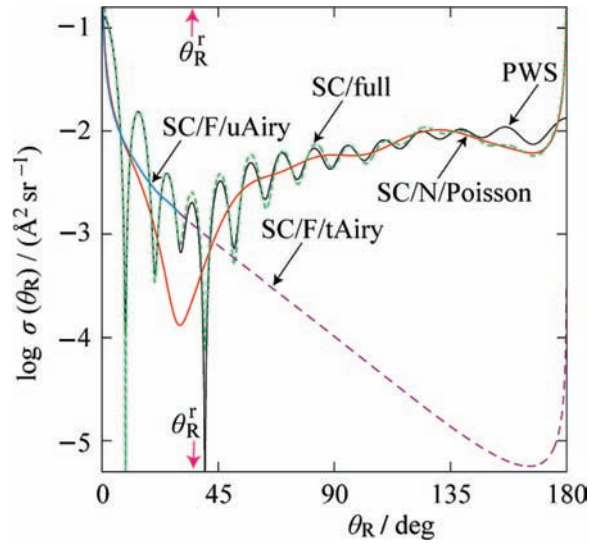

Figure 2. Plot of the logarithm of the differential cross section, log $\sigma(\theta_R)$, vs reactive scattering angle, θ_R. Black curve: full PWS DCS using eqs 1 and 2. Green dashed curve: full SC DCS using eqs 18 and 19. Blue curve: F uniform Airy SC DCS using eqs 20, 28−31. Purple dashed curve: F transitional Airy SC DCS using eqs 20, 32 and 33. Red curve: N Poisson SC DCS using eqs 20 and 23, together with quadrature applied to the integral $I_-(\theta_R)$ in eq 24. The two pink arrows indicate the rainbow singularity at $\theta_R^r = 35.2°$ which separates the bright side of the rainbow, $\theta_R < \theta_R^r$, from its dark side, $\theta_R > \theta_R^r$.

3. Results

In this section, we present and discuss our results for the N, F and full SC DCSs and LAMs, which we compare with the corresponding PWS quantities. We have also carefully checked that the approximations used in the three steps of the SC theory described in Section 2B are fully justified and numerically accurate.

A. Full PWS DCS and Farside, Nearside, and Full SC DCSs. Figure 2 plots the full PWS DCS (black curve, using eqs 1 and 2) on a logarithmic scale for the $F + H_2$ reaction using an accurate set of scattering matrix elements,[51,52] $\{\tilde{S}_J\}$ with $J = 0, 1, 2, ..., 23$ and $\tilde{S}_J \equiv 0$ for $J > 23$ for the Stark−Werner potential energy surface.[89] There are 24 partial waves contributing to the PWS, and the semiclassical theory developed in Section 2B is therefore applicable; that is, the reaction takes place under semiclassical conditions, $kR \gg 1$. We also note from the graph in Figure 1b that it is valid to assume $|\tilde{S}(J)|$ varies slowly with J. This has also been demonstrated earlier in ref 51.

There are two striking features in the PWS DCS: (1) an intense peak at forward angles − this is a *glory*, as has been proven by a uniform semiclassical analysis.[51,53,54,56,60] (2) *Diffraction oscillations* across the whole angular range; below, we prove they arise from the NF interference of a F Airy rainbow with the N scattering.

The two Airy curves, labeled SC/F/uAiry and SC/F/tAiry in Figure 2 and drawn blue and purple dashed, respectively, are

the uniform Airy and transitional Airy SC DCSs, respectively, for the F scattering. It can be seen that the rainbow is broad with the transition from the bright side to the dark side occurring at $\theta_R^r = 35.2°$ (indicated by a pink arrow on the upper and lower abscissae). We note that the transitional Airy DCS merges smoothly with the uniform Airy DCS; this tells us that the second-order Taylor expansion (eq 32) used in the derivation of the transitional Airy approximation[87] is, indeed, valid for $\theta_R \approx \theta_R^r$.The DCS calculated by the SC/F/Poisson approximation is similar to the Airy DCSs and is not displayed.

The red curve in Figure 2 is the N SC cross section, calculated by quadrature of the Poisson integral $I_-(\theta_R)$ in eq 24 and labeled SC/N/Poisson. It does not display any rapid oscillations; rather, it varies relatively slowly with θ_R. This behavior is analyzed further below. The minimum near $\theta_R = 30°$ probably arises from interference of the energy-domain analogues of time-direct and time-delayed scattering, since a similar minimum occurs in the N $R = 0$ PWS DCS of the $H + D_2(v_i = 0, j_i = 0) \rightarrow HD(v_f = 3, j_f = 0) + D$ reaction, which has been analyzed in detail in ref 61.

The dashed green curve in Figure 2 is the full SC DCS calculated using eqs 18 and 19. We see that it agrees very closely with the full PWS DCS for $1° \lesssim \theta_R \lesssim 150°$. This demonstrates the accuracy of the SC theory developed in Section 2B and proves that a F Airy rainbow does, indeed, contribute to the DCS in this angular range. Note that the rainbow actually dominates the angular scattering for $7° \lesssim \theta_R \lesssim 43°$, although the intensity of the full DCS in this range is smaller than in the two adjoining angular regions. This new rainbow is thus quite different in its properties from the rainbows normally encountered in molecular collisions.[32,36] The closest analogue is probably diffractive elastic scattering (as illustrated, for example, in Figures 4 and 5 of ref 90), where the F uniform Airy DCS is also broad, similar to the graph of $\sigma_+^{SC}(\theta_R)$ vs θ_R in Figure 2. Although our new rainbow has unusual properties, similar rainbows are expected to occur in the angular scattering of many state-to-state chemical reactions, since the SC analysis is generic and not specific to the present $F + H_2$ example.

B. Additional Discussion. Inspection of Figure 2 shows that the graph of $\sigma_-^{SC}(\theta_R)$ vs θ_R, computed by quadrature of the Poisson integral in eq 24 and labeled SC/N/Poisson, is almost monotonic for $\theta_R^{min} < \theta_R < \theta_R^{max}$. The reason for this can be seen in the plot of $|\tilde{S}(J)|$ vs J in Figure 1b: $|\tilde{S}(J)|$ is much larger at the inner stationary phase point than at the two outer stationary phase points when $\theta_R^{min} < \theta_R < \theta_R^{max}$. As a result, the inner stationary phase point is the major contributor to $f_-^{SC}(\theta_R)$, and there are no strong interferences. This is confirmed by evaluating $f_-^{SC}(\theta_R)$ using the primitive stationary phase approximation (PSA)[51] for the inner stationary phase point when $\theta_R^{min} < \theta_R < \theta_R^{max}$: The resulting N PSA SC DCS is very similar to the SC/N/Poisson curve in Figure 2.

We have also modified $|\tilde{S}(J)|$ in Figure 1b so that it is approximately bell-shaped, thereby increasing the contribution of the two outer stationary phase points. However the resulting PWS DCS still does not show pronounced interference structure for $\theta_R^{min} < \theta_R < \theta_R^{max}$ characteristic of the Pearcey canonical integral.[88] Evidently, to observe a pronounced cusped rainbow in the DCS requires more partial waves to contribute to the scattering, as is the case for the $He^+ + Ne$ example of ref 88.

The divergence in the SC DCSs at $\theta_R = 0°$ can be avoided by using a uniform SC glory theory, which agrees very closely with the full PWS DCS for $0° \leq \theta_R \lesssim 10°$ (see Figure 5 of ref 51). The discrepancies between $\sigma^{SC}(\theta_R)$ and $\sigma(\theta_R)$ for $\theta_R \gtrsim 150°$ arise mainly from neglect of the $m = -1$ term in the Poisson series representation for $f(\theta_R)$.

It was noted in Section 2B that the dominant contribution to $f_+^{tAiry}(\theta_R)$ comes from the term $Ai((\theta_R - \theta_R^r)/q_r^{1/3})$ in eq 33. Now, the first maximum of $Ai(x)$ occurs close to $x = -1.02$. Solving $(\theta_R - \theta_R^r)/q_r^{1/3} = -1.02$ for $\theta_R \in [-180°, 180°]$ gives for the position of the rainbow maximum, $\theta_R \approx -14°$. This value is outside the physical range of $\theta_R \in [0°, 180°]$ and emphasizes that the $F + H_2$ rainbow is a broad one.

A striking property of the F and N DCSs in Figure 2 is that F scattering dominates over the N scattering for $7° \lesssim \theta_R \lesssim 43°$. Now, F scattering usually arises from attractive forces and corresponds to surface waves (Regge states) that propagate around the reaction zone and decay into the forward direction[43,65] (in classical language, a short-lived rotating FHH complex). In contrast, the N scattering usually arises from repulsive interactions. It would be interesting to see if the relation between the potential energy surface and these two reaction mechanisms could be better understood by applying the plane wavepacket theory of time dependent scattering to the $F + H_2$ reaction and constructing its semiclassical limit (see refs 57 and 61 for an application to the $H + D_2$ reaction.)

C. Comparison of N, F Resummed PWS DCSs with N, F SC DCSs. In this section, we compare the NF $R = 0$ and $R = 1$ PWS DCSs with the corresponding NF SC DCSs. The NF PWS decompositions of eqs 4−6 for $R = 0$ or eqs 13 and 14 for $R = 1$ are not unique, and there is no guarantee that the resulting NF analysis of structure in the full PWS DCS is physically meaningful.[49] If possible, it is important to check whether the NF PWS decomposition being used is physically meaningful or not. Fortunately, we can do this for the $F + H_2$ reaction because in Section 2B, we derived the SC limits of the N and F subamplitudes, which are unique. We thus have a rare and valuable opportunity to assess the physical effectiveness of the Fuller NF PWS decomposition. Comparing the SC and PWS DCSs gives the following results:

(a) Comparison of Nearside Resummed PWS DCSs with the Nearside SC DCS. Both the N $R = 0$ (unresummed) and $R = 1$ (resummed) PWS DCSs calculated using eqs 7 and 15, respectively, agree very closely with the SC/N/Poisson DCS, which is drawn as a red curve in Figure 2. Because of this close agreement, the N $R = 0$ and $R = 1$ PWS DCSs are not shown separately in Figure 2.

(b) Comparison of Farside Resummed PWS DCSs with the Farside SC DCS. Figure 3 plots on a logarithmic scale the SC/F/uAiry DCS (blue curve) and the SC/F/tAiry DCS (purple dashed curve) joined at $\theta_R = 30°$ vs θ_R together with the PWS/F/$R = 0$ DCS (black curve) and the PWS/F/$R = 1$ DCS (blue dashed−dotted curve) calculated using eqs 8 and 16, respectively. We see that the F $R = 1$ PWS DCS agrees better with the Airy curve than does the F $R = 0$ PWS DCS, especially for $\theta_R \gtrsim 33°$. Observe that resummation of the PWS has removed from the F $R = 0$ PWS DCS some unphysical oscillations; this operation is called "cleaning".[49] Differences between the two F PWS curves and the Airy DCS are most pronounced at large angles. However, in this angular range, Figure 2 shows that $\sigma_+^{SC}(\theta_R) \ll \sigma_-^{SC}(\theta_R)$, so these differences are not physically significant because the numerical contribution of $f_F(\theta_R)$ to $f(\theta_R)$ is small. Note that the SC/F/tAiry DCS will itself have larger errors for $\theta_R \gg \theta_R^r$ because the second-order Taylor expansion (32) on which it is based is most reliable for $\theta_R \approx \theta_R^r$.

D. Comparison of N, F Resummed PWS LAMs with N, F SC LAMs. The LAMs provide information on the value of

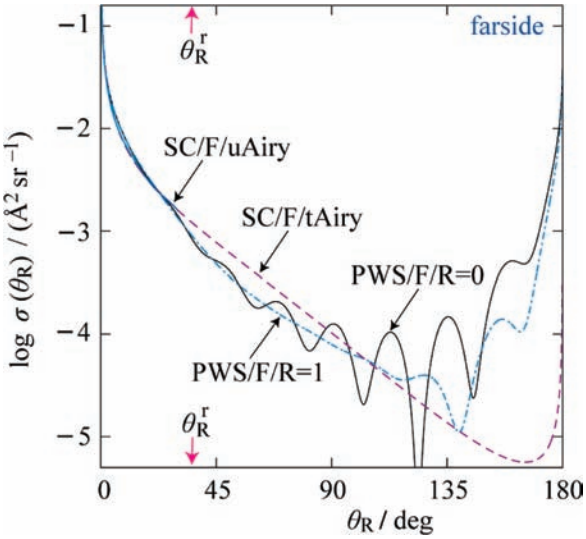

Figure 3. Plot of the logarithm of the differential cross section, log $\sigma_F(\theta_R)$ or log $\sigma_+^{SC}(\theta_R)$ for the farside scattering, vs reactive scattering angle, θ_R. Black curve: F $R = 0$ PWS DCS using eqs 5 and 8. Blue dashed−dotted curve: F $R = 1$ PWS DCS using eqs 14 and 16. Blue curve: F uniform Airy SC DCS using eqs 20 and 28−31. Purple dashed curve: F transitional Airy SC DCS using eqs 20, 32, and 33. The two pink arrows indicate the rainbow singularity at $\theta_R^r = 35.2°$, which separates the bright side of the rainbow, $\theta_R < \theta_R^r$, from its dark side, $\theta_R > \theta_R^r$.

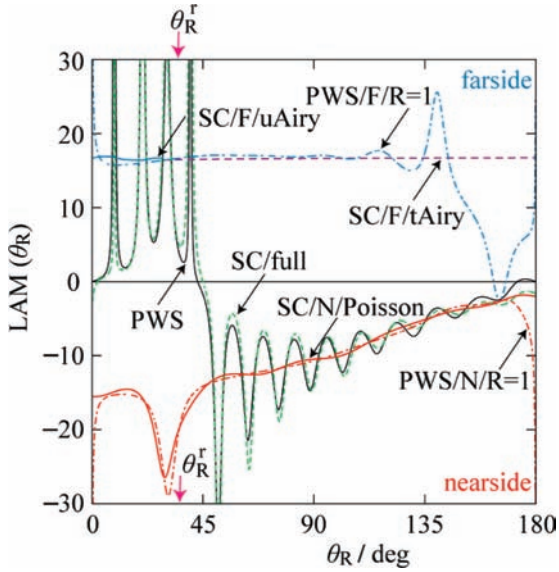

Figure 4. Plot of the local angular momentum, LAM(θ_R), vs reactive scattering angle, θ_R. Black curve: full PWS LAM(θ_R) using eqs 2 and 9. Blue dash-dot curve: F $R = 1$ PWS LAM using eqs 14 and 17. Red dashed−dotted curve: N $R = 1$ PWS DCS using eqs 14 and 17. Green dashed curve: full SC LAM using eq 21. Blue curve: F uniform Airy SC LAM using eqs 28−31 and 37. Purple dashed curve: F transitional Airy SC LAM using eqs 32, 33, and 38. Red curve: N Poisson SC LAM using eqs 21 and 23, together with quadrature applied to the integral $I_-(\theta_R)$ in eq 24. The two pink arrows indicate the rainbow singularity at $\theta_R^r = 35.2°$ which separates the bright side of the rainbow, $\theta_R < \theta_R^r$, from its dark side, $\theta_R > \theta_R^r$.

the total angular momentum variable that contributes to the scattering at an angle, θ_R.[49] In Figure 4, we compare the $R = 1$ PWS and SC LAMs, both full and N, F; see eqs 9 and 17. The SC LAMs are defined in a way analogous to the PWS LAMs; for example,

$$\mathrm{LAM}_+^{\mathrm{uAiry}}(\theta_R) = \frac{\mathrm{d}\arg f_+^{\mathrm{uAiry}}(\theta_R)}{\mathrm{d}\theta_R} \tag{37}$$

See also eq 21. Note that the N, F SC LAMs are unique.

The full SC and PWS LAMs in Figure 4 are similar, and their interference structure is consistent with the NF analysis of the DCSs in Figures 2 and 3. In addition, the N, F $R = 1$ PWS LAMs agree with the N, F SC LAMs, which provides another important check that the PWS NF decomposition is physically meaningful. Although The PWS/F/$R = 1$ LAM differs significantly from the SC/F/tAiry LAM for $\theta_R \gtrsim 110°$, this occurs in an angular region where $\sigma_F(\beta_1; \theta_R) \ll \sigma_N(\beta_1; \theta_R)$ (see Figures 2 and 3), so it is not physically significant. Note that PWS LAMs have previously been plotted and discussed in Figures 3a and 4a of ref 52 for $R = 0$, 1, and 2.

Inspection of Figure 4 shows that the F SC LAM is almost constant with angle. This can be understood by examining eq 33 for $f_+^{\mathrm{tAiry}}(\theta_R)$. Since the Ai(•) term dominates in eq 33, we have for the F SC LAM

$$\mathrm{LAM}_+^{\mathrm{tAiry}}(\theta_R) = \frac{\mathrm{d}\arg f_+^{\mathrm{tAiry}}(\theta_R)}{\mathrm{d}\theta_R} \approx \lambda_r = 16.9 \tag{38}$$

which is a constant, independent of θ_R.

The N LAMs in Figure 4 decrease in magnitude for $\theta_R \gtrsim 50°$, which is typical for a reaction that is dominated by repulsive interactions at large scattering angles.[52] The minima near $\theta_R = 30°$ probably arise from interference of the energy-domain analogues of time-direct and time-delayed scattering, since a similar minimum occurs in the N $R = 0$ PWS LAM of the H + D_2 ($v_i = 0$, $j_i = 0$) → HD ($v_f = 3$, $j_f = 0$) + D reaction.[61]

4. Conclusions

We have derived the semiclassical (asymptotic) limit of the scattering amplitude for the F + H_2 ($v_i = 0$, $j_i = 0$, $m_i = 0$) → FH ($v_f = 3$, $j_f = 3$, $m_f = 0$) + H reaction at a relative translational energy of 0.119 eV. We discovered a surprising new result: The angular scattering is an example of (attractive) rainbow scattering. We proved this result by showing that the (farside) semiclassical scattering subamplitude is characterized by an Airy function and its first-order derivative, with the transition from the bright side of the rainbow to its dark side occurring at $\theta_R = 35.2°$. The rainbow is broad, which explains why it has not been recognized in the many earlier theoretical and experimental studies. The rainbow reveals its presence by interference with the nearside scattering subamplitude, producing characteristic diffraction oscillations in the full DCS. We showed there is an angular region in the DCS where the rainbow dominates, but with the unusual property that it is less intense than in adjoining angular regions. Although the new rainbow has unusual properties, similar rainbows are expected to occur in the DCSs of many state-to-state chemical reactions, since the semiclassical analysis is generic and not specific to the F + H_2 reaction.

We also used the semiclassical results to test the physical effectiveness of the Fuller nearside−farside decomposition of the partial wave series for the scattering amplitude. We confirmed that the Fuller decomposition is physically meaningful for the F + H_2 reaction; moreover, the Fuller nearside−farside DCSs can be cleaned of some unphysical oscillations by a resummation of the partial wave series. We obtained similar results for the nearside-farside local angular momenta.

Acknowledgment. Support of this research by the UK Engineering and Physical Sciences Research Council is gratefully acknowledged.

Appendix

Here, we present the asymptotic formulas needed to evaluate the integral $I_+(\theta_R)$ in eq 24. In particular, we use results in section IIIG of ref 87, which are based on the rigorous asymptotic analysis of Chester et al.[91] We consider the integral

$$I(\alpha) = \int_{-\infty}^{\infty} g(x) \exp[\mathrm{i} f(\alpha, x)]\, \mathrm{d}x \qquad (A.1)$$

where α is a real parameter, $g(x)$ and $f(\alpha, x)$ are real valued functions, and $g(x)$ is slowly varying. We assume there exist two (real) points of stationary phase, $x_2(\alpha)$ and $x_3(\alpha)$, which are the solutions of $f'(\alpha, x) = 0$, and which coalesce at $x = x_r \equiv x_r(\alpha_r)$ when $\alpha = \alpha_r$. The convenient notations $x_i \equiv x_i(\alpha)$, $g_i \equiv g(x_i)$, $f_i \equiv f(\alpha,x_i)$, $f_i'' \equiv \mathrm{d}^2 f(\alpha, x)/\mathrm{d}x^2|_{x=x_i}$, etc., for $i = 2$, 3, r will be used in the following. It is also assumed that $g_i \neq 0$, ∞ and $f_i'' \neq \infty$.

The uniform Airy approximation for the case $f_2'' \leq 0$ and $f_3'' \geq 0$ is given by[87]

$$I^{\mathrm{uAiry}}(\alpha) = 2^{1/2}\pi \exp(\mathrm{i}A)\left\{\left[\frac{g_3}{(f_3'')^{1/2}} + \frac{g_2}{(-f_2'')^{1/2}}\right]\varsigma^{1/4}\mathrm{Ai}(-\varsigma) - \mathrm{i}\left[\frac{g_3}{(f_3'')^{1/2}} - \frac{g_2}{(-f_2'')^{1/2}}\right]\varsigma^{-1/4}\mathrm{Ai}'(-\varsigma)\right\} \qquad (A.2)$$

where

$$A(\alpha) = \frac{1}{2}(f_2 + f_3) \qquad (A.3)$$

and

$$\varsigma(\alpha) = \left[\frac{3}{4}(f_2 - f_3)\right]^{2/3} \qquad (A.4)$$

Note that $\varsigma(\alpha) \geq 0$. In eq A.2, the prime on the Airy function, $\mathrm{Ai}'(x)$, means $\mathrm{d}\,\mathrm{Ai}(x)/\mathrm{d}x$. If $\mathrm{Ai}(-\varsigma)$ and $\mathrm{Ai}'(-\varsigma)$ are replaced by their asymptotic approximations valid for $\varsigma \gg 1$ in eq A.2, then the primitive stationary phase result for $I(\alpha)$ is obtained.[87]

Equation A.2 becomes numerically indeterminate, 0/0, at the point of coalescence, where $f_2'' = f_3'' = f_r'' = 0$ and $\varsigma(\alpha) = 0$.To overcome this problem, we use the transitional Airy approximation, which is obtained by Taylor expanding $f(\alpha, x)$ to third order and $g(x)$ to first order, about $x = x_r$ in the integral in eq A.1. The result is[87]

$$I^{\mathrm{tAiry}}(\alpha) = 2\pi\left(\frac{2}{f_r'''}\right)^{1/3} \exp(\mathrm{i}f_r)\left[g_r \mathrm{Ai}\left(f_r'\left(\frac{2}{f_r'''}\right)^{1/3}\right) - \mathrm{i}g_r'\left(\frac{2}{f_r'''}\right)^{1/3}\mathrm{Ai}'\left(f_r'\left(\frac{2}{f_r'''}\right)^{1/3}\right)\right] \qquad (A.5)$$

Notice that eq A.5 can be used on both the bright and dark sides of the rainbow singularity because it only requires information on $g(x)$, $f(\alpha, x)$ and their derivatives at $x = x_r$.

The Airy rainbow formulas in Section 2 for the F SC subamplitude, $f_+^{\mathrm{SC}}(\theta_R)$, are obtained by making the identifications $\alpha \rightarrow \theta_R$, $x \rightarrow \lambda$, $x_i \rightarrow \lambda_i$ for $i = 2$, 3, r, $g(x) \rightarrow \lambda^{1/2}|\tilde{S}(\lambda)|$, and $f(\alpha,x) \rightarrow \arg \tilde{S}(\lambda) + \lambda\theta_R$ in eqs A.1−A.5.

References and Notes

(1) Yang, X. *Annu. Rev. Phys. Chem.* **2007**, *58*, 433.
(2) Hu, W.; Schatz, G. C. *J. Chem. Phys.* **2006**, *125* (132301), 1–15.
(3) Lin, S. Y.; Guo, H. *Phys. Rev. A* **2006**, *74* (022703), 1–8.
(4) Zhang, D. H. *J. Chem. Phys.* **2006**, *125* (133102), 1–4.
(5) Yuan, K.; Cheng, Y.; Liu, X.; Harich, S.; Yang, X.; Zhang, D. H. *Phys. Rev. Lett.* **2006**, *96* (103202), 1–4.
(6) Hankel, M.; Smith, S. C.; Allan, R. J.; Gray, S. K.; Balint-Kurti, G. G. *J. Chem. Phys.* **2006**, *125* (164303), 1–12.
(7) Gómez-Carrasco, S.; Roncero, O. *J. Chem. Phys.* **2006**, *125* (054102), 1–14.
(8) Chu, T.-S.; Han, K.-L.; Hankel, M.; Balint-Kurti, G. G. *J. Chem. Phys.* **2007**, *126* (214303), 1–9.
(9) Koszinowski, K.; Goldberg, N. T.; Zhang, J.; Zare, R. N.; Bouakline, F.; Althorpe, S. C. *J. Chem. Phys.* **2007**, *127* (124315), 1–10.
(10) Lin, S. Y.; Guo, H.; Honvault, P.; Xu, C.; Xie, D. *J. Chem. Phys.* **2008**, *128* (014303), 1–8.
(11) Banks, S. T.; Clary, D. C. *Phys. Chem. Chem. Phys.* **2007**, *9*, 933.
(12) Lin, S. Y.; Bañares, L.; Guo, H. *J. Phys. Chem. A* **2007**, *111*, 2376.
(13) Rusin, L. Yu.; Sevryuk, M. B.; Toennies, J. P. *Khim. Fiz.* **2007**, *26*, 11, No. 8. [English translation: *Russ. J. Phys. Chem. B*, **2007**, *1*, 452.]
(14) Bargueño, P.; González-Lezana, T.; Larrégaray, P.; Bonnet, L.; Rayez, J.-C.; Hankel, M.; Smith, S. C.; Meijer, A. J. H. M. *J. Chem. Phys.* **2008**, *128* (244308), 1–14.
(15) De Fazio, D.; Aquilanti, V.; Cavalli, S.; Aguilar, A.; Lucas, J. M. *J. Chem. Phys.* **2008**, *129* (064303), 1–8.
(16) Sun, Z.; Zhang, D. H.; Xu, C.; Zhou, S.; Xie, D.; Lendvay, G.; Lee, S.-Y.; Lin, S. Y.; Guo, H. *J. Am. Chem. Soc.* **2008**, *130*, 14962.
(17) Lin, S. Y.; Guo, H. *J. Chem. Phys.* **2008**, *129* (124311), 1–9.
(18) Hankel, M.; Smith, S. C.; Gray, S. K.; Balint-Kurti, G. G. *Comput. Phys. Commun.* **2008**, *179*, 569.
(19) Sun, Z.; Lin, X.; Lee, S.-Y.; Zhang, D. H. *J. Phys. Chem. A* **2009**, *113*, 4145.
(20) Chu, T.-S.; Han, K.-L.; Hankel, M.; Balint-Kurti, G. G.; Kuppermann, A.; Abrol, R. *J. Chem. Phys.* **2009**, *130* (144301), 1–9.
(21) Espinosa-García, J.; Nyman, G.; Corchado, J. C. *J. Chem. Phys.* **2009**, *130* (184315), 1–9.
(22) Remmert, S. M.; Banks, S. T.; Clary, D. C. *J. Phys. Chem. A* **2009**, *113*, 4255.
(23) Sun, Z.; Lee, S.-Y.; Guo, H.; Zhang, D. H. *J. Chem. Phys.* **2009**, *130* (174102), 1–11. Erratum: *J. Chem. Phys.* **2009**, *131*, 049906, pp 1−2.
(24) Neumark, D. M.; Wodtke, A. M.; Robinson, G. N.; Hayden, C. C.; Lee, Y. T. *J. Chem. Phys.* **1985**, *82*, 3045.
(25) Wang, X.; Dong, W.; Qiu, M.; Ren, Z.; Che, L.; Dai, D.; Wang, X.; Yang, X.; Sun, Z.; Fu, B.; Lee, S.-Y.; Xu, X.; Zhang, D. H. *Proc. Natl. Acad. Sci. U.S.A.* **2008**, *105*, 6227.
(26) Child, M. S. *Molecular Collision Theory*; Dover Publications: Mineola, New York, USA, 1996. (An unabridged and unaltered republication of the 1984 corrected reprinting of the work first published by Academic Press, London and New York, 1974, as Volume 4 of the monograph series "Theoretical Chemistry".)
(27) Connor, J. N. L. In *Semiclassical Methods in Molecular Scattering and Spectroscopy*; Child, M. S., Ed.; Proceedings of the NATO ASI held in Cambridge, England in September 1979; Reidel: Dordrecht, Holland, 1980; pp 45−107.
(28) Brink, D. M.; *Semiclassical Methods for Nucleus−Nucleus Scattering*; Cambridge University Press: Cambridge, UK, 1985.
(29) Child, M. S. *Semiclassical Mechanics with Molecular Applications*; Clarendon Press: Oxford, UK, 1991.
(30) Nussenzveig, H. M. *Diffraction Effects in Semiclassical Scattering*; Cambridge University Press: Cambridge, UK, 1992.
(31) Grandy, W. T. *Scattering of Waves from Large Spheres*; Cambridge University Press: Cambridge, UK, 2000.
(32) Adam, J. A. *Phys. Rep.* **2002**, *356*, 229.
(33) Connor, J. N. L.; McCabe, P.; Sokolovski, D.; Schatz, G. C. *Chem. Phys. Lett.* **1993**, *206*, 119.
(34) Sokolovski, D.; Connor, J. N. L.; Schatz, G. C. *Chem. Phys. Lett.* **1995**, *238*, 127.
(35) Sokolovski, D.; Connor, J. N. L.; Schatz, G. C. *J. Chem. Phys.* **1995**, *103*, 5979.
(36) McCabe, P.; Connor, J. N. L. *J. Chem. Phys.* **1996**, *104*, 2297.
(37) Sokolovski, D.; Connor, J. N. L.; Schatz., G. C. *Chem. Phys.* **1996**, *207*, 461.
(38) Wimp, J.; McCabe, P.; Connor, J. N. L. *J. Comput. Appl. Math.* **1997**, *82*, 447.

(39) McCabe, P.; Connor, J. N. L.; Sokolovski, D. *J. Chem. Phys.* **1998**, *108*, 5695.
(40) Sokolovski, D.; Connor, J. N. L. *Chem. Phys. Lett.* **1999**, *305*, 238.
(41) Hollifield, J. J.; Connor, J. N. L. *Phys. Rev. A* **1999**, *59*, 1694.
(42) Hollifield, J. J.; Connor, J. N. L. *Mol. Phys.* **1999**, *97*, 293.
(43) Dobbyn, A. J.; McCabe, P.; Connor, J. N. L.; Castillo, J. F. *Phys. Chem. Chem. Phys.* **1999**, *1*, 1115.
(44) Vrinceanu, D.; Msezane, A. Z.; Bessis, D.; Connor, J. N. L.; Sokolovski, D. *Chem. Phys. Lett.* **2000**, *324*, 311.
(45) McCabe, P.; Connor, J. N. L.; Sokolovski, D. *J. Chem. Phys.* **2001**, *114*, 5194.
(46) Whiteley, T. W. J.; Noli, C.; Connor, J. N. L. *J. Phys. Chem. A* **2001**, *105*, 2792.
(47) Noli, C.; Connor, J. N. L.; Rougeau, N.; Kubach, C. *Phys. Chem. Chem. Phys.* **2001**, *3*, 3946.
(48) Noli, C.; Connor, J. N. L. *Russ. J. Phys. Chem.* **2002**, *76*, S77; Supplement 1; also available at http://arXiv.org/abs/physics/0301054.
(49) Anni, R.; Connor, J. N. L.; Noli, C. *Phys. Rev. C* **2002**, *66*, 044610.
(50) Anni, R.; Connor, J. N. L.; Noli, C. *Khim. Fiz.* **2004**, *23*, 6; No. 2; also available at http://arXiv.org/abs/physics/0410266.
(51) Connor, J. N. L. *Phys. Chem. Chem. Phys.* **2004**, *6*, 377.
(52) Connor, J. N. L.; Anni, R. *Phys. Chem. Chem. Phys.* **2004**, *6*, 3364.
(53) Connor, J. N. L. *Mol. Phys.* **2005**, *103*, 1715.
(54) Xiahou, C.; Connor, J. N. L. In *Semiclassical and Other Methods for Understanding Molecular Collisions and Chemical Reactions*; Sen, S., Sokolovski, D., Connor, J. N. L., Eds.; (Collaborative Computational Project on Molecular Quantum Dynamics (CCP6), Daresbury Laboratory: Warrington, UK, 2005); pp 44−49; ISBN 0-9545289-3-X.
(55) Monks, P. D. D.; Connor, J. N. L.; Althorpe, S. C. In *Semiclassical and Other Methods for Understanding Molecular Collisions and Chemical Reactions*; Sen, S., Sokolovski, D., Connor, J. N. L., Eds.; (Collaborative Computational Project on Molecular Quantum Dynamics (CCP6), Daresbury Laboratory: Warrington, UK, 2005); pp 112−118; ISBN 0-9545289-3-X.
(56) Xiahou, C.; Connor, J. N. L. *Mol. Phys.* **2006**, *104*, 159.
(57) Monks, P. D. D.; Connor, J. N. L.; Althorpe, S. C. *J. Phys. Chem. A* **2006**, *110*, 741.
(58) Monks, P. D. D.; Xiahou, C.; Connor, J. N. L. *J. Chem. Phys.* **2006**, *125* (133504), 1–13.
(59) Monks, P. D. D.; Connor, J. N. L.; Althorpe, S. C. *J. Phys. Chem. A* **2007**, *111*, 10302.
(60) Connor, J. N. L.; Shan, X.; Totenhofer, A. J.; Xiahou, C. In *Multidimensional Quantum Mechanics with Trajectories*; Shalashilin, D. V., de Miranda M. P., Eds.; (Collaborative Computational Project on Molecular Quantum Dynamics (CCP6), Daresbury Laboratory: Warrington, UK, 2009); pp 38−47; ISBN 978-0-9545289-8-0.
(61) Monks, P. D. D.; Connor, J. N. L.; Bouakline, F. *J. Phys. Chem. A* **2009**, *113*, 4746.
(62) Schatz, G. C. In *Advances in Classical Trajectory Methods*; Hase, W. L. Ed.; JAI Press: Stamford, CT, 1998; Vol. 3; pp 205−229.
(63) Nyman, G.; Yu, H.-G. *Rep. Prog. Phys.* **2000**, *63*, 1001.
(64) Sokolovski, D. *Russ. J. Phys. Chem.* **2002**, *76*, S21; Supplement 1.
(65) Sokolovski, D.; Castillo, J. F.; Tully, C. *Chem. Phys. Lett.* **1999**, *313*, 225.
(66) Sokolovski, D.; Castillo, J. F. *Phys. Chem. Chem. Phys.* **2000**, *2*, 507.
(67) Sokolovski, D. *Phys. Rev. A* **2000**, *62* (024702), 1–4.
(68) Aoiz, F. J.; Bañares, L.; Castillo, J. F.; Sokolovski, D. *J. Chem. Phys.* **2002**, *117*, 2546.
(69) Sokolovski, D. *Chem. Phys. Lett.* **2003**, *370*, 805.
(70) Sokolovski, D.; Msezane, A. Z. *Phys. Rev. A* **2004**, *70* (032710), 1–12.
(71) Sokolovski, D.; Sen, S. K.; Aquilanti, V.; Cavalli, S.; De Fazio, D. *J. Chem. Phys.* **2007**, *126* (084305), 1–11.
(72) Sokolovski, D.; Msezane, A. Z.; Felfli, Z.; Ovchinnikov, S. Yu.; Macek, J. H. *Nucl. Instrum. Methods Phys. Res. B* **2007**, *261*, 133.
(73) Sokolovski, D. *Phys. Rev. A* **2007**, *76* (042125), 1–13.
(74) Sokolovski, D. *Phys. Scr.* **2008**, *78* (058118), 1–9.
(75) Juanes-Marcos, J. C.; Althorpe, S. C.; Wrede, E. *Science* **2005**, *309*, 1227. For a commentary, see Clary, D. C. *Science* **2005**, *309*, 1195.
(76) Juanes-Marcos, J. C.; Althorpe, S. C.; Wrede, E. *J. Chem. Phys.* **2007**, *126* (044317), 1–11.
(77) Panda, A. N.; Althorpe, S. C. *Chem. Phys. Lett.* **2007**, *439*, 50.
(78) Althorpe, S. C.; Juanes-Marcos, J. C.; Wrede, E. *Adv. Chem. Phys.* **2008**, *138*, 1.
(79) Bouakline, F.; Althorpe, S. C.; Ruiz, D. P. *J. Chem. Phys.* **2008**, *128* (124322), 1–12.
(80) Guillon, G.; Stoecklin, T. *Euro. Phys. J. D* **2006**, *39*, 359.
(81) Stoecklin, T.; Voronin, A.; Dham, A. K.; Stoker, J. S.-F.; McCourt, F. R. W. *Mol. Phys.* **2008**, *106*, 75.
(82) Greaves, S. J.; Murdock, D.; Wrede, E. *J. Chem. Phys.* **2008**, *128* (164307), 1–8.
(83) Greaves, S. J.; Murdock, D.; Wrede, E.; Althorpe, S. C. *J. Chem. Phys.* **2008**, *128* (164306), 1–10.
(84) Greaves, S. J.; Wrede, E.; Goldberg, N. T.; Zhang, J. Y.; Miller, D. J.; Zare, R. N. *Nature* **2008**, *454*, 88. For a commentary, see Brouard, M. *Nature* **2008**, *454*, 43.
(85) Goldberg, N. T.; Zhang, J. Y.; Miller, D. J.; Zare, R. N. *J. Phys. Chem. A* **2008**, *112*, 9266.
(86) Fuller, R. C. *Phys. Rev. C* **1975**, *12*, 1561.
(87) Connor, J. N. L.; Marcus, R. A. *J. Chem. Phys.* **1971**, *55*, 5636. For a commentary, see Connor, J. N. L. *Current Contents: Physical, Chemical and Earth Sciences* **1991**, *31*, 10, No. 50. Connor, J. N. L. *Current Contents: Engineering, Technology and Applied Sciences* **1991**, *22*, 10; No. 50; also available at http://garfield.library.upenn.edu/classics1991/A1991GR14400001.pdf.
(88) Connor, J. N. L.; Farrelly, D. *J. Chem. Phys.* **1981**, *75*, 2831.
(89) Stark, K.; Werner, H.-J. *J. Chem. Phys.* **1996**, *104*, 6515.
(90) Connor, J. N. L.; Farrelly, D.; Mackay, D. C. *J. Chem. Phys.* **1981**, *74*, 3278.
(91) Chester, C.; Friedman, B.; Ursell, F. *Proc. Camb. Phil. Soc.* **1957**, *53*, 599. Reprinted in *Ship Hydrodynamics, Water Waves and Asymptotics, Collected Papers of F. Ursell, 1946−1992*; Ursell, F. Ed.; World Scientific: Singapore, 1994; Vol. II; pp 708−720. For a commentary, see *Ship Hydrodynamics, Water Waves and Asymptotics, Collected Papers of F. Ursell, 1946−1992*; Ursell, F., Ed.; World Scientific: Singapore, 1994; Vol. II; p 570.

JP906042G